Tellus (1987), *39A*, 307–325

The synoptic climatology of polar-low outbreaks over the Gulf of Alaska and the Bering Sea

By STEVEN BUSINGER, *Department of Marine, Earth and Atmospheric Sciences, North Carolina State University, Raleigh, NC 27695-8208, USA*

(Manuscript received 14 June 1986; in final form 21 January 1987)

ABSTRACT

The synoptic environments conducive to the development of polar-low outbreaks are investigated for the North Pacific region, including the Gulf of Alaska and the Bering Sea. Two case studies of polar low outbreaks are presented, using standard synoptic data, all available ship reports and satellite imagery. One case occurred over the Bering Sea, and the other over the Gulf of Alaska. The case studies show that the environments conducive to the development of strong polar lows include: a deep outflow of arctic air over open water and a cold-core, closed low aloft. Additionally, forcing from a small-scale vortex aloft is associated with the formation of strong polar lows. When synoptic conditions are favorable for the formation of polar lows, a series of them often develop in close proximity to each other. Furthermore, once favorable environmental conditions have developed, they often persist for several days and can result in several polar-low outbreaks.

To develop a climatology of the synoptic environments conducive to the formation of polar lows over the Gulf of Alaska, 500 mb height, temperature, 1000–500 mb thickness and surface pressure data were composited for days when mature polar lows were present. The composite studies reveal the presence of significant negative anomalies centered over the northern Gulf of Alaska in the 500 mb temperature, height and thickness fields. These results indicate the presence of enhanced positive vorticity and the potential for deep convection over the area.

The evolution of the negative-height anomaly indicates the development of a trough that results in a northerly component of the flow aloft over the Aleutian Islands and Alaska Peninsula as much as three days prior to the outbreak of polar lows. Strong northerly surface flow across open water indicated by the surface pressure composite results in small static stabilities at low levels and in the development of baroclinicity in the boundary layer through the modifying effects of surface fluxes of sensible and latent heat. Finally, a comparison is made between the climatology of polar lows over the Gulf of Alaska and over the Norwegian and Barents Seas.

1. Introduction

In recent years, increasing attention has been given to cyclonic vortices that form in polar-air masses. These vortices occur most often over the oceans in winter, originating in regions of enhanced convection and developing a comma- or spiral-shaped cloud pattern as they mature. The rapid development and small scale of the disturbances make them difficult to forecast. Baroclinicity through some or all of the troposphere, and conditional instability through a substantial depth, are two forms of instability that coexist in the wide spectrum of cyclonic vortices. Accordingly, researchers have divided these disturbances into two broad categories (Rasmussen, 1981, 1983; Reed and Blier, 1986a, b): comma clouds; larger comma-shaped cloud systems (>500 km in diameter) that form in closer proximity to major frontal boundaries, in which slantwise baroclinic ascent is the dominant driving force (Reed, 1979; Reed and Blier, 1986a, b), and polar lows; smaller spiral-shaped systems that form deep in the cold airmasses, in which

convection and arctic fronts, separating modified from unmodified boundary-layer air, are thought to be important (Rasmussen, 1981, 1983; Shapiro and Fedor, 1986). Since polar lows and comma clouds are part of a continuous range of disturbances, there is a grey area in the nomenclature in which a disturbance could be called either a polar low or a comma cloud. A possible example of this may be the case described by Harrold and Browning (1969), for which satellite imagery was unavailable.

Studies of comma clouds that occurred over the Eastern Pacific Ocean, have shown that these disturbances form in regions of enhanced tropospheric baroclinicity, usually near major preexisting frontal boundaries, and on the cyclonic shear side of strcng (>55 m s^{-1}) upper-tropospheric jet streams (Mullen, 1979; Locatelli, Hobbs and Werth, 1982). The incipient stage of comma clouds is associated with enhanced convection, which often assumes a banded character as the storm matures (Businger, 1986). In the latter stages of development, the distinctive comma-shaped cloud pattern seen in satellite imagery is primarily composed of stratiform clouds (generally associated with baroclinic ascent), and is coincident with a region of differential positive-vorticity advection (Reed, 1979). In strong storms, the mesoscale temperature-advection patterns can appear indistinguishable from those associated with fronts in typical midlatitude cyclones (Locatelli et al., 1982). For a further discussion of comma clouds the reader is referred to Reed and Blier (1986a, b). The remainder of this paper is concerned with the characteristics of polar lows over the Northern Pacific Ocean, the Gulf of Alaska, and the Bering Sea, and the evolution of the synoptic environment conducive to their formation.

Studies of polar lows over the north Atlantic Ocean and Norwegian Sea have shown that these storms form at high latitudes during the movement of arctic air over warm oceans, under the influence of cold-core lows at 500 mb (Mansfield, 1974; Rasmussen, 1983; Businger, 1985; Reed and Duncan, 1987). Imagery from polar-orbiting satellites, reveals polar lows as small (<500 km in diameter), spiral-shaped cloud patterns. Embedded within these cloud patterns are cellular features with cold radiative cloud-top temperatures (<-40°C, indicative of enhanced convective activity) around a central core that is often clear (Rasmussen, 1985b; Shapiro, Fedor and Hampel, 1987).

It has long been known that the North Atlantic region, including the Norwegian and Barents Seas, is a prolific breeding ground for polar lows (Rabbe, 1975; Rasmussen, 1977, 1981). Satellite imagery has, however, shown that there are a number of high-latitude regions where polar lows commonly appear in winter. Regions where open water is in close proximity to snow- or ice-covered surfaces are especially predisposed to the formation of polar lows.

The northern Gulf of Alaska and the Bering Sea are regions over which small-scale (<500 km in diameter), spiral-shaped storms are often observed, yet there are virtually no references to these disturbances in the literature. In this study, infrared-satellite photographs from the polar-orbiting NOAA-4 through NOAA-7 satellites were carefully inspected. Days on which vigorous polar lows (exhibiting a well-developed spiral cloud structure and high cloud tops indicated by cold radiative cloud-top temperatures) were present over these regions were noted. Fig. 1

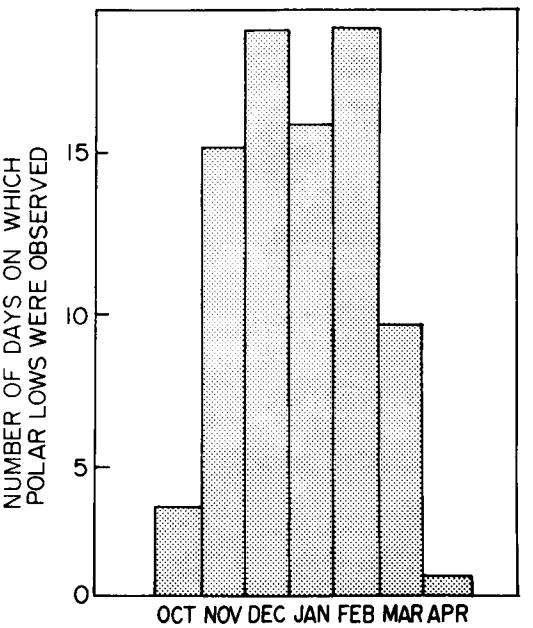

Fig. 1. Histogram of the number of days per month on which polar lows were observed in polar-orbiting satellite imagery over the Gulf of Alaska or the Bering Sea during the period 1975–1983.

shows a histogram of the number of days per month that polar lows were observed over the Gulf of Alaska or the Bering Sea during the period 1975 through 1983. In analyzing the satellite imagery for Fig. 1, it was found that in ~20% of the "polar-low" days more than one polar low was observed in the satellite imagery. On these days the polar lows tended to form in a series in close proximity to one another, analogous to the cyclone families described by Bjerknes and Solberg (1922), but on a shortened time scale. (It should be noted in Fig. 1 that the totals given reflect the number of days on which polar lows were observed; therefore, these statistics may underestimate the actual number of polar lows that occurred.) Furthermore, ~35% of the polar-low days were followed by polar low developments within 48 hours, suggesting that once environmental conditions conducive to the formation of polar lows occur they tend to persist for several days.

Fig. 2 shows the sea-surface temperature distribution and the mean position of the ice edge in winter for the Gulf of Alaska and the eastern Bering Sea. The tongue of warmer water just off the coast in the northern Gulf of Alaska is a result of the advection of warm water northward along the coast by the Alaska current (Royer, 1975). Also note the sea-surface temperature gradient (up to ~4°C) across the Alaska Peninsula. The asterisks in Fig. 2 indicate the geographic locations of the centers of the spiral-cloud signatures associated with the polar lows in the satellite imagery over the Gulf of Alaska. The distribution of the asterisks shows that polar-low development is favored over the northern Gulf of Alaska within ~500 km of the coast.

In Section 2, case studies of polar-low outbreaks over the Gulf of Alaska and Bering Sea will be presented. In Section 3, synoptic data from the National Meteorological Center (NMC) are composited in order to obtain a climatology of the environments in which polar lows develop over the Gulf of Alaska. The superposed-epoch method of analysis (see Businger, 1985) is used to composite the data. In the final section of this paper, the climatology of polar lows occurring over the Gulf of Alaska is compared with the climatology of those occurring over the Norwegian and Barents Seas.

2. Two case studies of polar lows

Two case studies of polar-low outbreaks are presented below to document the synoptic scale

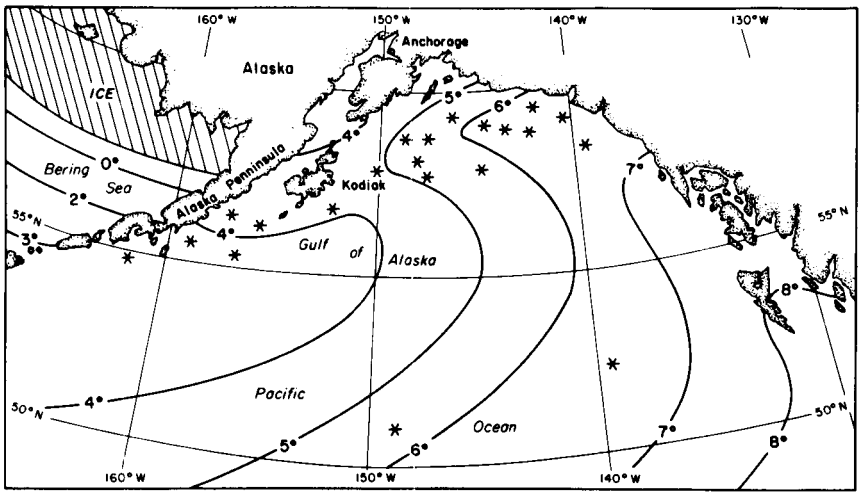

Fig. 2. Mean sea-surface temperature (°C) and mean extent of the 5/8 sea-ice concentration (hatched area) for the Gulf of Alaska and eastern Bering Sea; 20-year mean (1957–1978) for January (from the US Department of Interior's Bureau of Land Management). The asterisks indicate the geographic locations of the centers of the spiral-cloud signatures associated with polar lows in the satellite imagery.

characteristics of the surface pressure fields and the 500 mb height and temperature fields associated with polar lows over the Gulf of Alaska and the Bering Sea, and to provide a broader background from which to evaluate the results of the composite studies given in Section 3.

2.1. Case 1

In January 1979, an extended cold-core low at 500 mb dominated the Bering Sea for approximately seven days. During this period, a number of polar lows developed.

The infrared image given in Fig. 3 shows the characteristic spiral-cloud structure of a mature polar low. This image was taken by the NOAA-5 polar orbiting satellite over the Bering Sea and Kamchatka Peninsula at 22.24 GMT on 23 January 1979. The diameter of the head of the cloud spiral was ~300 km, smaller than cloud shields typically associated with comma clouds (Reed, 1979), and much smaller than those

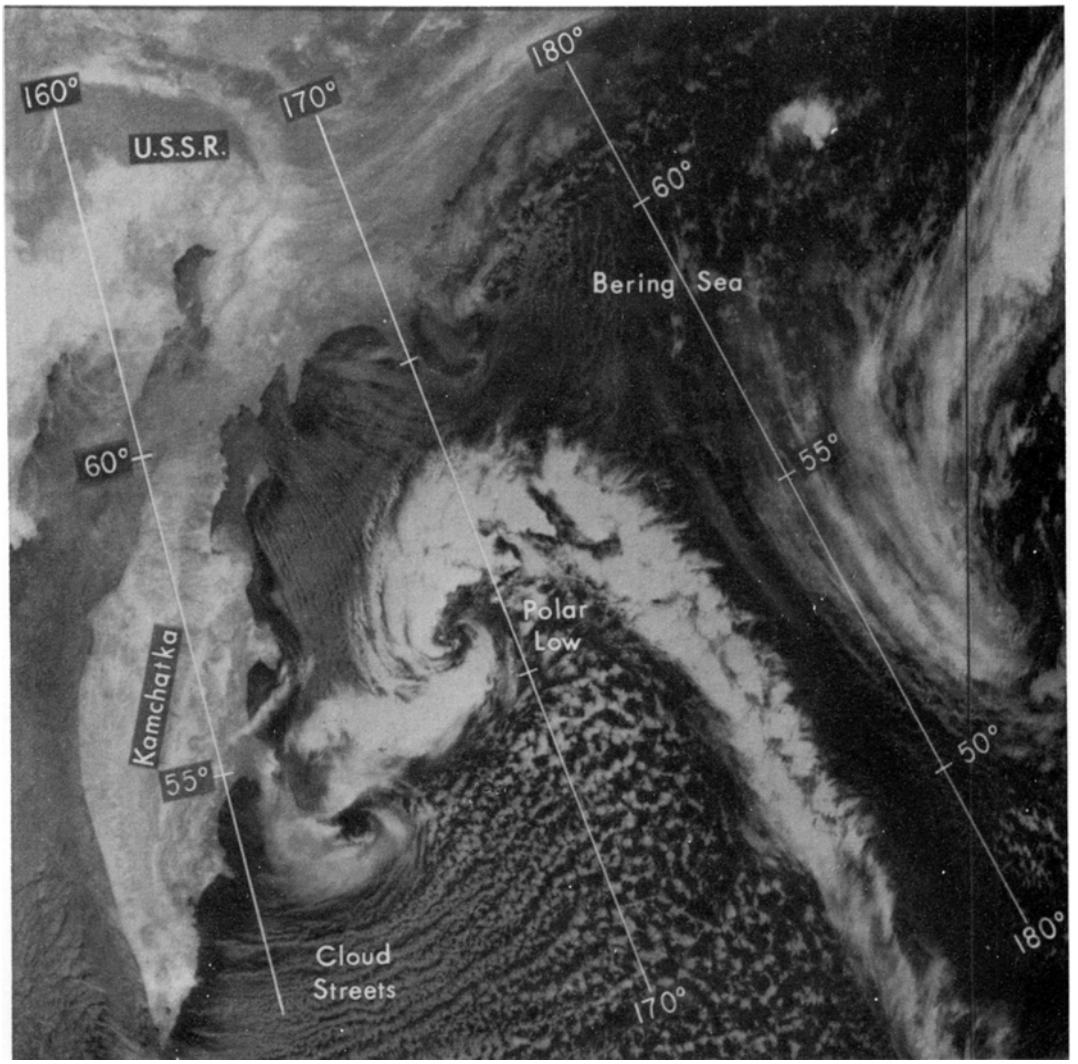

Fig. 3. NOAA-5 infrared satellite photograph of a polar low and cloud streets over the Bering Sea at 22.24 GMT on 23 January 1979.

associated with mid-latitude cyclones. Cloud streets can be seen to the east of Kamchatka streaming toward the polar low, as cold air flows from the ice-covered surface to the west over open water in the western Bering Sea. It can be inferred from the signature of the clouds in Fig. 3 that the cloud band extending from the polar low southward was the leading edge of the arctic outbreak (Shapiro and Fedor, 1986) and, thus, may represent an arctic front. A smaller incipient vortex can be seen in the clouds to the south of the polar low.

The synoptic events leading to this polar-low outbreak are depicted in figs. 4 and 5. For several days prior to this development the Bering Sea was dominated by a broad, cold-core low and light winds at 500 mb (Fig. 4). Approximately 24 hours previous to the satellite image (Fig. 3), a small vortex (~500 km diameter) and very low temperatures can be seen at 500 mb over the southern tip of Kamchatka (Fig. 4a). At this time (00.00 GMT, 23 January 1979) the surface analysis (Fig. 5a) shows a trough of low pressure extending northeast along the coast to a low-pressure center associated with a slowly filling occlusion over the northern Bering Sea. There is evidence in the surface data that baroclinicity was generated in the boundary layer in the vicinity of this trough by differential heating of the boundary-layer air (Rasmussen, 1985b; Shapiro and Fedor, 1986). The air to the west of the trough experienced a short trajectory over the water, while air east of the trough had a much longer trajectory over open water. Temperatures on the Kamchatka coast were between −16 and −23°C (Fig. 5a), whereas, to the east the temperatures ranged from −2 to −6°C. During the following 24 hours the 500 mb vortex moved northeastward (Fig. 4b). A reduction in the static stabilty likely resulted as increasingly cold air aloft moved over boundary-layer air that had been warmed and moistened by fluxes from the sea surface.

Rawindsonde data for Ostrov Bering Island were unavailable for the period of interest. However, as a way of estimating the potential for deep convection (Reed and Blier, 1985b), a lifted index can be computed for the vicinity of Ostrov Bering Island at 00.00 GMT on 24 January 1979. An air parcel warmed to near 2°C with a dew-point temperature of ~0°C at 990 mb (the sea-surface temperature was near 4°C along Ostrov

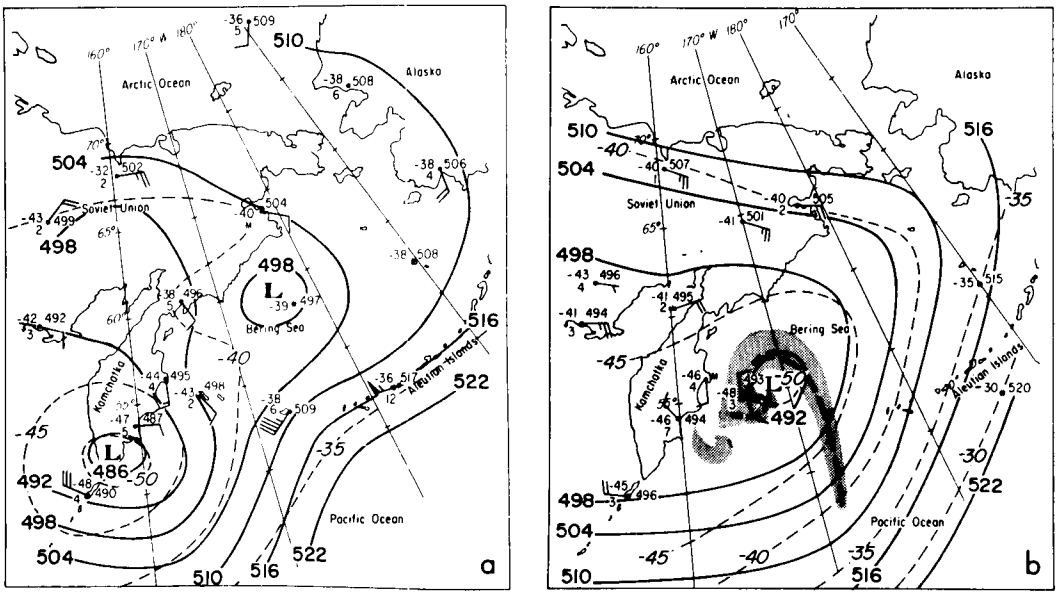

Fig. 4. Geopotential analyses for: (a) 00.00 GMT 23 January 1979, and (b) 00.00 GMT 24 January 1979, showing 500 mb heights (solid contours, interval 60 m) and temperatures (dashed contours, interval 5°C). Shaded regions in (b) indicate the approximate extent of the cloud cover derived from satellite photographs.

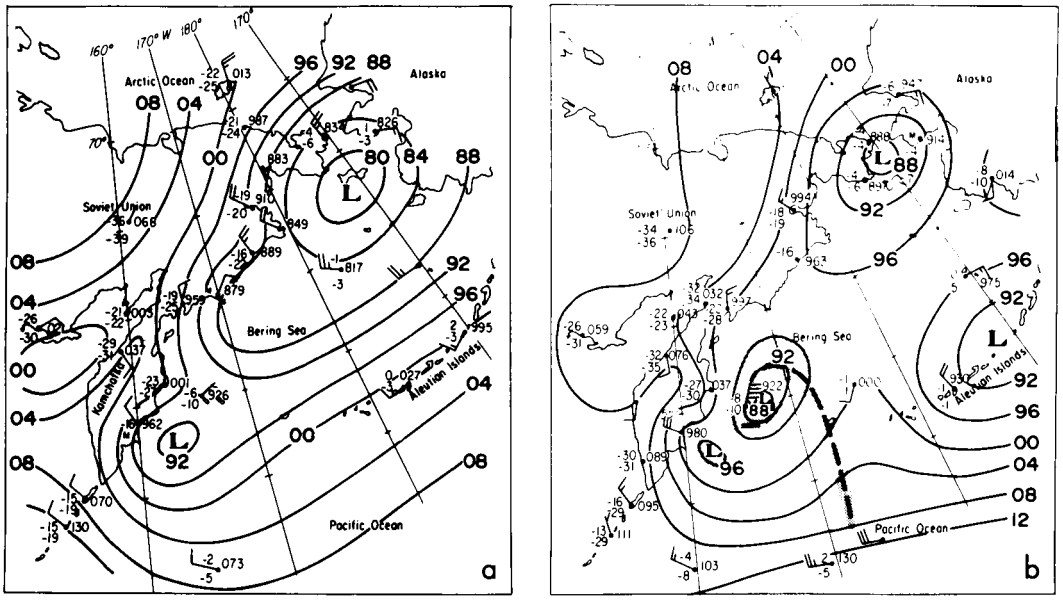

Fig. 5. Surface analyses for (a) 00.00 GMT 23 January 1979, and (b) 00.00 GMT 24 January 1979. Solid contours are surface pressure every 4 mb. Shaded regions in (b) indicate the approximate extent of the cloud cover derived from satellite photographs.

Bering Island during January 1979) would experience a temperature surplus of ~9°C after rising dry and then moist adiabatically to 500 mb where the environmental temperature was −48°C (Fig. 4b). This corresponds to a lifted index of −9, indicating the potential for deep convection at a time when the signature of convective activity was observed in the satellite imagery (Fig. 3).

The quasi-geostrophic omega equation (Holton, 1979) shows that differential positive-vorticity advection (PVA) results in rising motions in the middle troposphere, leading to cyclone or vortex development at the surface (Sutcliff, 1947). Thus, PVA associated with the small 500 mb vortex may have provided a favorable environment in which the incipient storm could organize into a mature polar low.

Fig. 5b shows the surface analysis for 00.00 GMT 24 January 1979 (close to the time of the satellite image in Fig. 3). A tight low with closed isobars has now formed just east of Kamchatka, with station Nikolskoe on Ostrov Island reporting steady surface winds of 20 m s^{-1} from the northeast. The dimensions of the outermost closed isobar was ~300 × 500 km. By contrast, the surface-pressure signature of a mature occluded cyclone could occupy the entire Bering Sea. During the following 12 hours, satellite imagery showed that another polar low formed along the Kamchatka Coast to the north of the first disturbance.

2.2. *Case 2*

In Fig. 6, a well-defined polar low is visible over the northern Gulf of Alaska. This infrared image, taken by the NOAA 6 polar orbiting satellite at 20.21 GMT on 22 March 1975, shows the eastern Bering Sea and the northern Gulf of Alaska. Analyses of synoptic and satellite data show that two polar lows formed on this day (we will refer to these as polar lows #1 and #2). Polar low #1 is well-defined in the satellite image (Fig. 6), while polar low #2 formed from the merging of convective elements seen to the south of polar low #1 during the four hours following the time of the satellite image.

For several days prior to this polar-low outbreak moderately strong northerly winds (10–15 m s^{-1}) at the surface resulted in the formation of cloud streets. The cloud streets extended from the ice edge in the Bering Sea and Bristol Bay

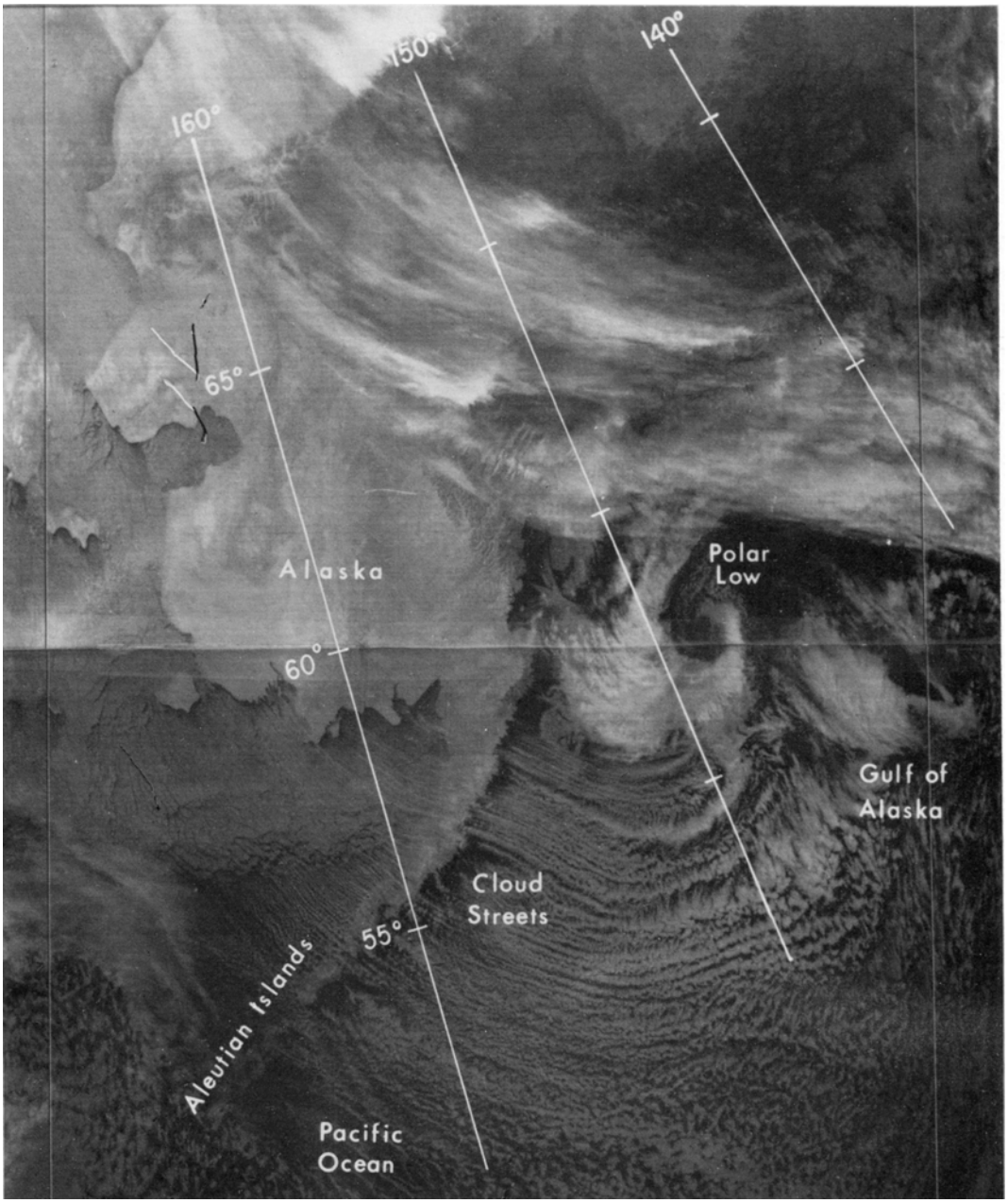

Fig. 6. NOAA-4 infrared satellite photograph of polar low and cloud streets over the Gulf of Alaska at 20.21 GMT on 22 March 1975.

across the Aleutian Islands. They gradually widened and became increasingly convective as they curved into the Gulf of Alaska (see Fig. 6). Prior to March 22, several small vortices were seen to form near the southern extent of the cloud streets; however, they remained shallow features that rapidly decayed before gaining appreciable strength. During this period a broad trough at the

500 mb level was slowly moving southward over Alaska. On 22 March a small 500 mb vortex (on the scale of a polar low, <500 km in diameter) within the upper-level trough migrated southeastward across western Alaska (Figs. 7a, b). Very cold air aloft (< −45°C) was associated with this feature. As the vortex crossed Kodiak Island, the 500 mb temperature dropped to −46°C.

Polar low #1 rapidly formed just south of Kodiak Island, as the 500 mb vortex passed over the open water of the Gulf of Alaska. Polar low #2 formed a few hours later in a region of enhanced tropospheric baroclinicity on the southern side of the 500 mb vortex. It should be noted that the deeper tropospheric baroclinicity present over the region in which polar low #2 formed is a characteristic of incipient comma clouds. This polar vortex, therefore, falls in a gray area of the nomenclature and could alternatively be classified as a comma cloud.

The surface-pressure analysis for 00.00 GMT 22 March (Fig. 8a) shows northerly winds of 10 to 15 m s^{-1} across the Aleutian Islands and the Alaska Peninsula. This flow brought arctic air into the Gulf of Alaska where fluxes of sensible and latent heat rapidly modified the boundary layer air (Shapiro and Fedor, 1986). Evidence for this modification can be seen in the increase in temperature and dew-point temperature with increasing distance south of the Alaska Peninsula (Fig. 8a). Generally light winds and rising pressures occupied the northeastern Gulf of Alaska, with an old occlusion tracking southeastward toward Washington State still visible in the lower right corner of Fig. 8a.

The surface analysis for 00.00 GMT 23 March (Fig. 8b) shows a general trough of low pressure over the northern Gulf of Alaska. This larger pressure trough has a scale characteristic of mid-latitude cyclones. Within this region two small centers of low pressure (~500 km in diameter) are associated with the two polar lows (central pressure ~980 mb for polar low #1 and ~984 mb for polar low #2). At this time a band of strong surface winds extended from the Aleutian Islands southwest across the Gulf of Alaska to the southeast coast of Alaska, with steady westerly winds of up to 25 m s^{-1} reported along the south side of polar low #2.

Fig. 9 shows four rawindsonde soundings taken at Kodiak, Alaska (located on the northwest side of Kodiak Island, see Fig. 2) at 12 hour intervals,

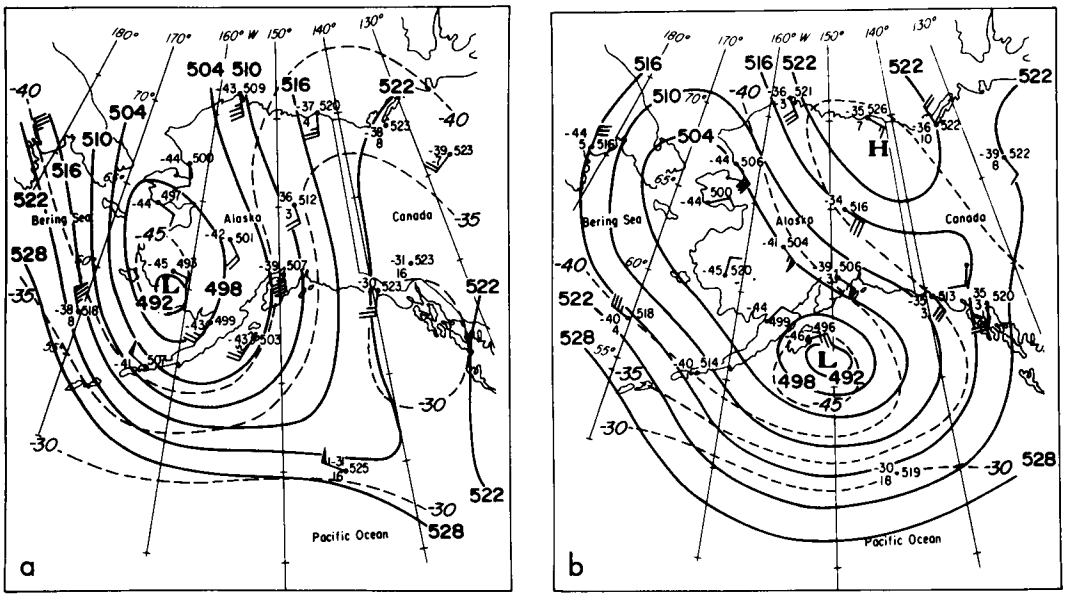

Fig. 7. Geopotential analyses for : (a) 00.00 GMT 22 March 1975, and (b) 00.00 GMT 23 March 1975, showing 500 mb heights (solid contours, interval 60 m) and temperatures (dashed contours, interval 5°C).

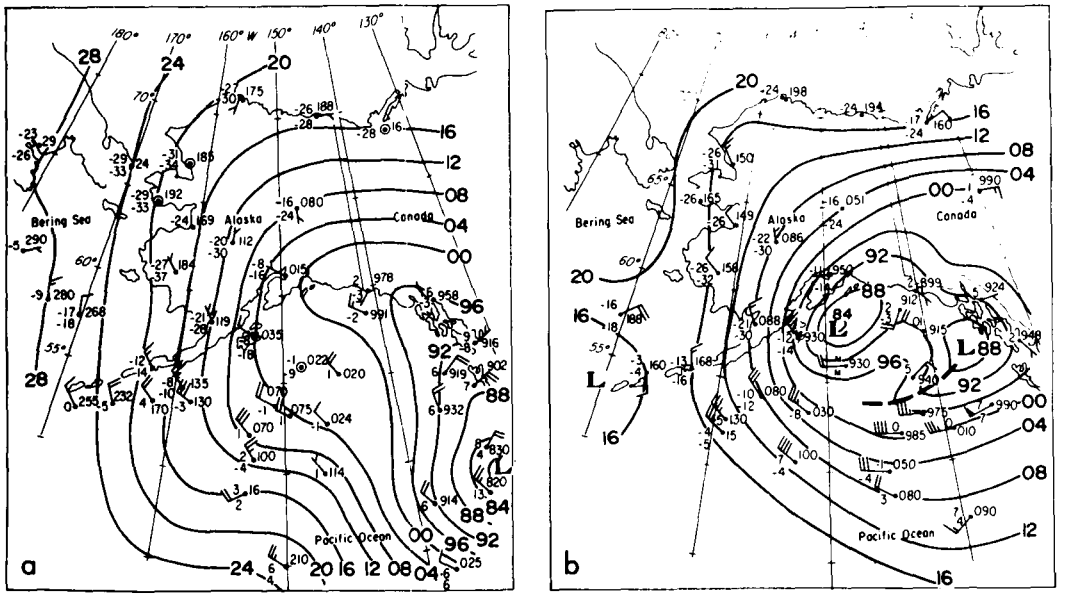

Fig. 8. Surface analyses for (a) 00.00 GMT 22 March 1975, and (b) 00.00 GMT 23 March 1975. Solid contours are surface pressure every 4 mb.

starting at 00.00 GMT 21 March. Kodiak is located ~250 km to the east of the polar low #1 in the satellite image (Fig. 6). The proximity of the rawindsonde ascents to polar low #1 allows features relevant to its development to be analysed.

The 12.00 GMT sounding on 21 March (Fig. 9a) is dry and stable throughout the troposphere. There is some backing of the wind barbs with height below 900 mb indicating cold advection near the surface at Kodiak, with little windshear above this level to 500 mb. Backing of the wind barbs with height indicates cold advection, assuming that the winds are in thermal-wind balance (Holton, 1979). By 00.00 GMT 22 March (Fig. 9b) pronounced backing of the wind barbs with height is seen in the layer from 950 to 850 mb. The 850 mb temperature cooled 5°C to −21°C in response to the cold advection during the 12 hours since the previous sounding (Fig. 9a). This has resulted in a conditionally unstable lapse rate form the surface to ~850 mb at this time. The dew-point temperature shows an increase in moisture with a layer of saturated air appearing in the southwest flow just above 850 mb. Speed shear in the winds between ~850 mb and ~550 mb is in response to the approach of the upper-level, cold-core trough. The sounding shows that the position of the tropopause is depressed to ~450 mb.

The sounding for 12.00 GMT on 22 March (Fig. 9c) shows a marked increase in the relative humidity at mid-levels in the troposphere, with saturated dew-point temperatures and predominantly southerly winds between ~920 and ~720 mb. The wind barbs show backing from ~950 mb to ~550 mb at this time. The backing of the wind is especially pronounced in the layer between 900 and 800 mb, over which there is directional change of almost 180°, and the conditional instability persists below 850 mb. At 500 mb the winds have turned from southwest to southeast and the temperature has lowered to −45°C, reflecting the proximity of the upper-level vortex.

The sounding for 00.00 GMT 23 March (Fig. 9d) shows an increase in the windspeed to ~13 m s^{-1} at the surface and ~15 m s^{-1} at 950 mb, with ~10 m s^{-1} at 700 mb. The occurrence of the strongest winds at low levels in polar lows has been noted previously in the literature (Rasmussen, 1977, 1985), and has been ascribed

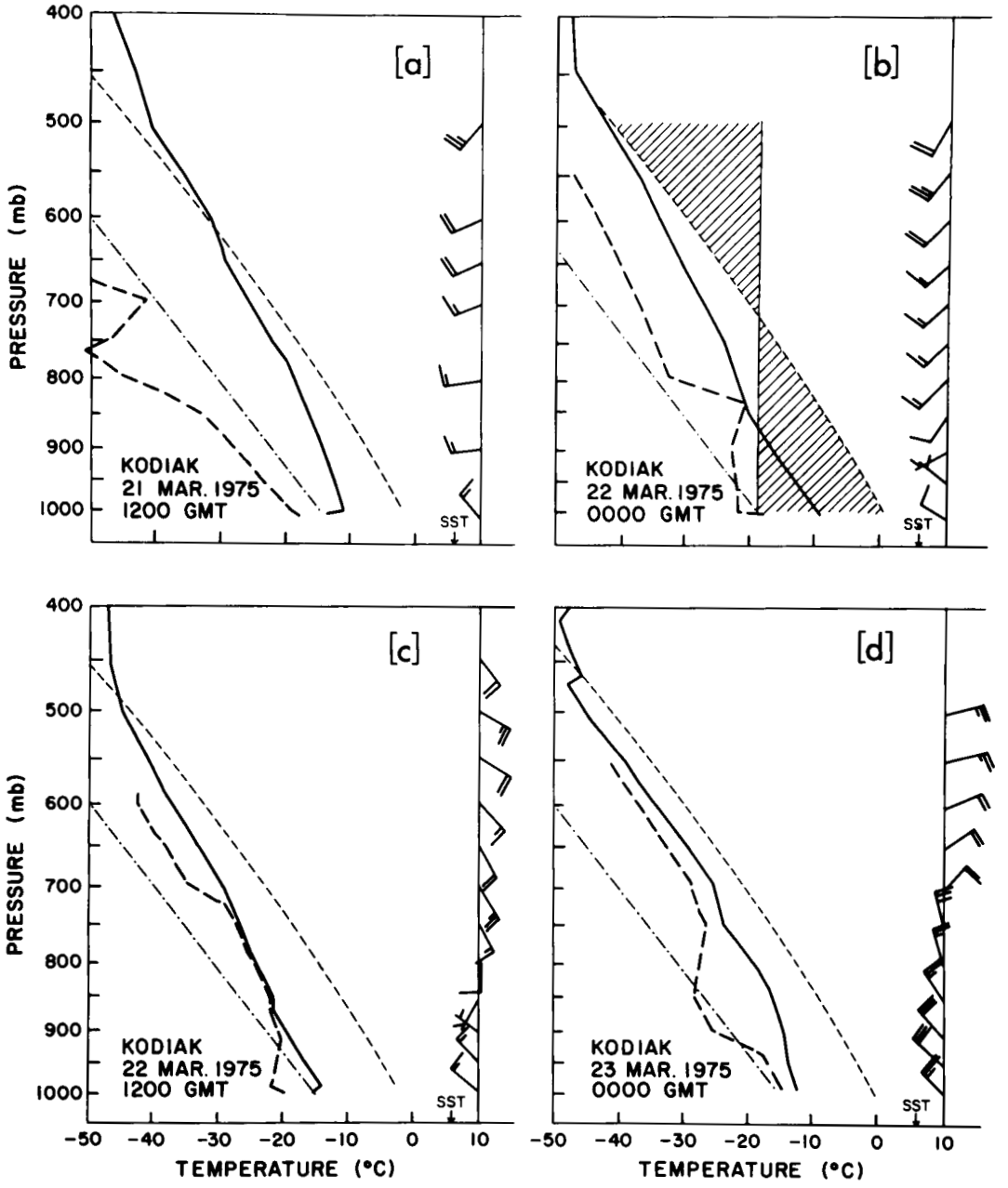

Fig. 9. Rawindsonde Soundings for Kodiak, Alaska at (a) 12.00 GMT 21 March 1975, (b) 00.00 GMT 22 March 1975, (c) 12.00 GMT 22 March 1975, (d) 00.00 GMT 23 March 1975. The temperature and dew-point profiles are indicated (in °C) by the heavy solid and dashed lines, respectively. Dry adiabats are shown as dash-dot lines, moist adiabats as thin dashed lines. Winds: half barb 2.5 m s^{-1}, full barbs 5 m s^{-1}. The shaded region in (b) illustrates the graphical technique used to calculate the mean-virtual temperature below 500 mb (see text).

to the presence of a core of warm air at low levels in these disturbances. Veering of the wind barbs in the layer from ~900 mb to 550 mb indicates general warm advecton. The temperature sounding shows warming at all levels below 500 mb, with an increase in the 850 mb temperature of almost 6°C in the 12 hours since the previous sounding (Fig. 9c). Furthermore, the temperature sounding is close to moist adiabatic above 700 mb, while having stabilized significantly below this level since the previous sounding. The dew-point profile shows an increase in relative humidity above 700 mb (close to saturated with respect to ice) from the previous sounding and a pronounced decrease below this level, with a dew-point temperature spread of more than 12°C at 850 mb. The resulting "onion shape" of this sounding is reminiscent of soundings taken in post-squall regions in the tropics (e.g., see Fig. 8 in Zipzer, 1977). In the tropical cases it was deduced that the low dew-point temperature air found behind the squall line just above the mixed layer resulted when dry air in the surroundings descended in mesoscale unsaturated downdrafts. The implication may be that the signature seen in the sounding data (Fig. 9d) is the result of organized subsidence that occurs below the upper-level cloud shield seen in the satellite image (Fig. 6) to the east of the surface low-pressure center. It is suggested that this subsidence may act to compensate for mesoscale ascent associated with the convergent circulation of polar low #1.

To diagnose the influence of the sensible- and latent-heat fluxes from the ocean surface on the development of polar low #1, some simple calculations can be made using the sounding data at Kodiak. The sea-surface temperature in the region southeast of Kodiak Island over which polar low #1 formed ranges from 4°C to 6°C (Fig. 2). As discussed above, cold dry air originating over continental Alaska is rapidly modified as it passes over the water. The result is a well-mixed boundary layer in which the surface-air temperature asymptotically approaches that of the sea surface and the depth of the mixed layer increases with increasing distance away from the coast/ice edge (Rasmussen, 1985b). To determine the time scale of this modification for the case of polar low #1, we will estimate the time needed to transform the temperature profile below 850 mb at 00.00 GMT on 22 March (Fig. 9b) to moist neutral with an air temperature of ~ -1°C at sea-level (corresponding to the moist adiabat in Fig. 9b), given a sea-surface temperature of ~4°C. (Note that a saturated air parcel warmed to ~ -1°C at sea level would experience a lifted index of ~ -2 when lifted to 500 mb). Equating the surface sensible-heat flux, using a bulk-aerodynamic formula, to the change in mean temperature in the boundary-layer we can write:

$$\rho c_p h \frac{dT}{dt} = \rho c_p C_d V(T_s - T),$$

where ρ = density of the air, c_p = specific heat at constant pressure, T = mean temperature below 850 mb, C_d = drag coefficient, V = wind speed, T_s = sea-surface temperature and h = geopotential height of the 850 mb surface.

Integrating from the surface to 850 mb we can write:

$$t = -\frac{h}{C_d V} \ln \frac{T_f - T_s}{T_0 - T_s},$$

where T_0 = initial mean temperature below 850 mb (taken from the Kodiak sounding at 00.00 GMT on March 22) and T_f = final mean temperature below 850 mb after the modification (taken from the moist adiabat shown in Fig. 9b). Using $T_0 = 257$ K, $T_f = 270$ K, $U = 15$ m s^{-1}, $C = 0.002$, $h = 1300$ m, we find that $t = 4.5 \times 10^4$ s, or ~12 hours.

The resulting estimate of 12 hours for the time needed to modify the mean temperature of the atmosphere below 850 mb is consistent with the development time for polar low #1 and is in agreement with time scales more generally associated with polar-low development (Rasmussen, 1981, 1985; Shapiro and Fedor, 1986).

We can estimate the sea-level pressure that would result if there exists within the polar low circulation an area of moist ascent approximately along the moist adiabat shown in Fig. 9b. Using a form of the hypsometric equation (Wallace and Hobbs, 1977), we can write:

$$P_{sfc} = p_z \exp \frac{g_0 Z}{R_d T_v},$$

where P_{sfc} = sea-level pressure, $p_z = 500$ mb, Z = height of the 500 mb geopotential surface (a

value of 5030 m was taken from the sounding), g_0 = gravitational acceleration, R_d = gas constant for dry air and T_v = mean-virtual temperature of the atmosphere in the layer from the surface to 500 mb. A value of 255 K for T_v was obtained graphically from the sounding (see Fig. 9b). After substitution, the result of 980 mb for the surface pressure agrees well with the analyzed value for the central sea-level pressure of polar low #1 (Fig. 8b).

In summary, these calculations suggest that the time scales of the boundary-layer modification by surface fluxes of sensible heat are consistent with observed time scales for polar-low development over the north Pacific region. Furthermore, the potential warming of an air column in the core of the polar-low circulation as a result of the surface fluxes of sensible and latent heat can account for the observed deepening at the surface.

2.3. Discussion of the case studies

In the case studies described above, polar low outbreaks occurred when winds in a deep layer advected cold arctic air from ice- or snow-covered regions over open water and a cold-core, closed low was present aloft. Additionally, differential PVA associated with a small-synoptic scale vortex at 500 mb may have provided a favorable environment in which the incipient storms could develop into mature polar lows (Sutcliffe, 1947; Holton, 1979).

A common element of incipient polar lows appears to be the presence of a weak surface trough (Fig. 7a) (Rasmussen, 1985a; Businger, 1985) and low-level baroclinicity (inferred from station and ship data) resulting from the modification of boundary-layer air by surface fluxes of latent and sensible heat as it was advected over the open water. It is likely that this modification also resulted in a decrease in the static stability of the atmosphere, especially at low levels (Shapiro and Fedor, 1986). Evidence from the sounding data and estimates of the lifted indices in the vicinity of the polar lows showed that there was a potential for deep convection. Satellite imagery showed the signature of deep convection surrounding the storm centers (Figs. 3, 6) consistent with previous case studies (Rasmussen, 1985a; Businger, 1985).

The outbreak of convective activity along the surface trough at the time of most rapid deepening suggests that there may be cooperation between the baroclinic and convective components of polar lows. A lack of detailed boundary layer and upper level data over the northern Pacific Ocean makes it difficult to assess the degree to which baroclinic versus convective processes contributed to the formation of these disturbances. However, analytical work by Mak (1982) has shown that baroclinic forcing in a disturbance can organize the condensational heating on a scale similar to the wave itself, resulting in significantly enhanced growth rates and a reduced wavelength of the most unstable mode (about one-third the dry model value).

As discussed in this section, two important characteristics of polar lows are the small horizontal dimensions of the perturbations and the potential for deep convection in the environment. Baroclinic theory (Eady, 1949) predicts that small static stability enhances the development of baroclinic waves while reducing the wavelength of the most unstable mode. Theoretical and numerical studies (Mansfield, 1974; Staley and Gall, 1977; Duncan, 1977; Satyamurty, Rao and Moura, 1982) show that small static stabilities at low levels favor a subsynoptic scale for most rapid baroclinic development. Sounding data for the polar low outbreak over the Gulf of Alaska (Fig. 9) showed small static stabilities at low levels in the environment of the polar lows. Small static stabilities at low levels were also indicated by the convective cloud streets seen in the satellite imagery (Figs. 3, 6) (Shapiro and Fedor, 1986).

Latent heat released in the convection observed in the case studies may also have contributed to the rapid growth and short wavelengths of the polar lows. Takioka (1973) showed that convective adjustment processes, resulting in latent heat release, tend to increase the warm temperature perturbations at mid-tropospheric levels. This results in a deeper disturbance while favoring the development of small-synoptic scale wavelengths. Numerical work by Sardie and Warner (1985) has shown that convective and non-convective latent heating and surface fluxes of sensible and latent heat were required to adequately simulate the development of a polar low over the Norwegian Sea.

Previous case studies have shown that the scale of polar lows is small (generally <500 km) and

their life cycle short (< 12 hours) (Businger, 1985; Rasmussen, 1985a). The case studies presented in this section show that when synoptic conditions are favorable for the formation of polar lows (winds advecting cold air from ice-covered regions over open water and the presence of a cold-core low aloft) a series of storms may develop in close proximity to each other, analogous to the cyclone families described by Bjerknes and Solberg (1922), but on a shortened time scale. Moreover, once environmental conditions favorable for the formation of polar lows have developed they often persist and can result in several consecutive days on which polar lows occur.

3. Superimposed-epoch analysis

The 500 mb charts (Fig. 4, 7) presented in the previous section provide evidence that there is a small-synoptic scale vortex and very cold temperatures (< −45 °C) in the upper troposphere at the time polar lows develop. To further investigate the relationship of the 500 mb height and temperature fields to formation of polar lows, a compositing of NMC data was undertaken for a number of well-developed polar lows observed over the northern Gulf of Alaska. Since this region is of limited extent (see Fig. 2), polar lows that form there lend themselves to analysis by "superposed-epoch method" (Panofsky and Brier, 1965). Following this method, dates were noted for all polar lows that developed to a mature stage over the northern Gulf of Alaska during the period from 1975 through 1983; these were termed "key days". Infrared satellite photographs from the polar orbiting NOAA-4 through NOAA-7 satellites were carefully inspected. Only days on which vigorous polar lows (exhibiting a well-developed spiral cloud structure and high cloud tops indicated by cold radiative cloud-top temperatures) were present within the prescribed region were designated as key days (e.g., Fig. 6) (Table 1). The locations of the centers of the cloud spirals associated with these storms are given in Fig. 2. The NMC 500 mb height data for the northern hemisphere for each of the key days were averaged to obtain a 500 mb "polar low climatology" for that region. An anomaly map was then computed by subtracting the seasonal mean 500 mb height field (see Businger, 1985) from the polar-low climatology field, thus indicating where the height field was above or below the seasonal mean during outbreaks of polar lows. The 500 mb height-anomaly field for the key day for this study is given in Fig. 10f.

Table 1. *Key days designated on the basis of satellite data over the Gulf of Alaska*

13 Feb. 1975	13 Dec. 1979
22 March 1975	21 Dec. 1979
8 Nov. 1975	27 Dec. 1979
12 Nov. 1975	15 Jan. 1980
26 Nov. 1975	6 March 1981
12 Nov. 1977	30 Oct. 1981
11 Dec. 1977	6 Dec. 1981
25 Nov. 1978	19 Feb. 1982
19 Jan. 1979	26 Feb. 1982
7 Feb. 1979	25 Dec. 1982
21 Nov. 1979	

Using the same procedure described above, the anomaly field for each day during an eleven day window centered on the key day was computed to show the evolution of the anomaly pattern from five days prior to five days after the outbreak (Fig. 10). Additionally, the 500 mb temperature, 1000–500 mb thickness and surface-pressure data were composited to complete a "synoptic-scale climatology" for the key days (Fig. 11).

Before discussing the results, two cautionary notes: first, as pointed out in Businger (1985), the data used in the compositing studies have insufficient resolution (grid spacing ~ 380 km) to adequately represent details of the atmospheric structure on the scale of an individual polar low. The purpose of the compositing studies is to gain insights into the larger synoptic-scale environments in which these storms occur. Second, the distribution of key days used in the composites favor the months of November through March (Table 1), while the period October through April was used to compute the seasonal mean. This may have resulted in a slight bias in the anomaly fields presented in Section 4.

4. Discussion of results

Fig. 10 shows the time evolution of a striking height-anomaly pattern over the Northern Gulf of Alaska at the 500 mb level. On the key day

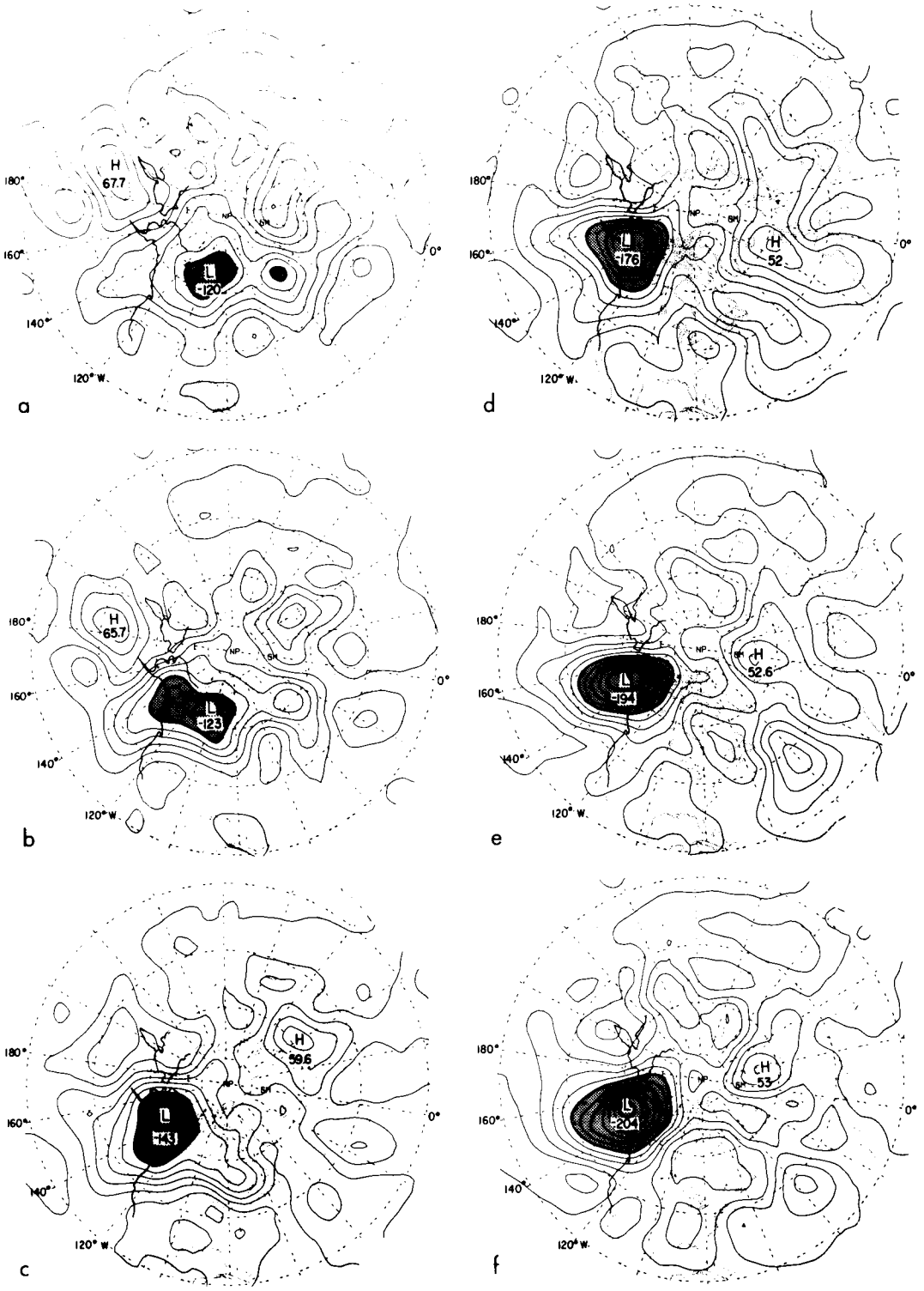
a
H
67.7
L
-120
b
H
65.7
L
-123
c
H
59.6
L
-131
d
L
-176
H
52
e
L
-194
H
52.6
f
L
-204
cH
53
180°
160°
140°
120° W.
0°
NP
SH

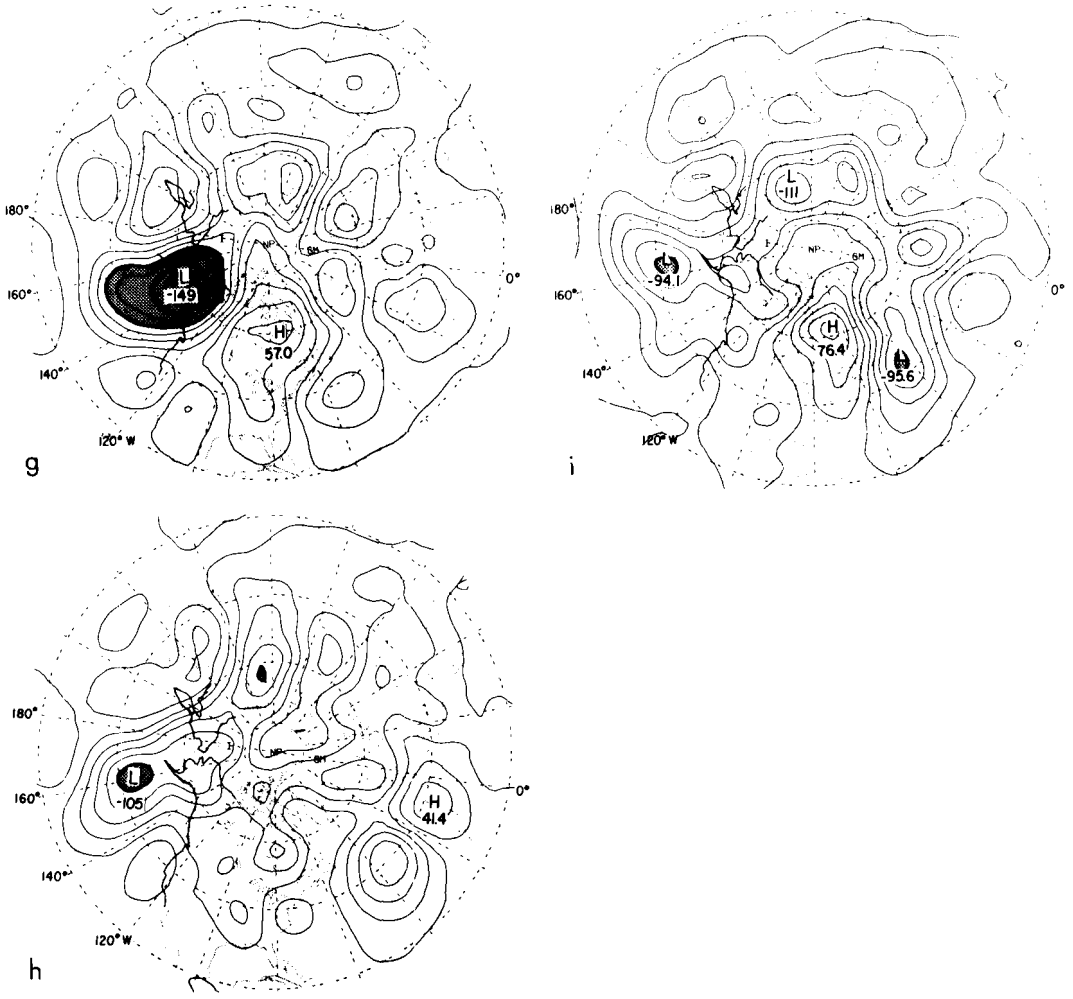

Fig. 10. Evolution of the 500 mb anomaly field (contour interval 20 m) for 21 cases over the Gulf of Alaska, 1975–1983: (a) key day − 5, (b) key day − 4, (c) key day − 3, (d) key day − 2, (e) key day − 1, (f) key day, (g) key day + 1, (h) key day + 3, (i) key day + 5. Shaded regions indicate negative-height anomalies more than 80 m below the winter seasonal mean.

(Fig. 10f) the pattern indicates that a 500 mb trough was located just south of Kodiak Island, with a northerly component to the geostrophic flow over the Alaska Peninsula and the Aleutian Islands.

The pronounced negative-height anomaly near Kodiak Island (200 m below the winter season mean) is evidence for the presence of enhanced positive vorticity over the region. It is interesting to compare the signature of the negative-anomaly pattern (Fig. 10f) with the 500 mb height chart (Fig. 7b). Note the similarity in placement and shape of the trough and anomaly patterns.

The evolution of the 500 mb anomaly pattern (Fig. 10) shows a westward motion early in the sequence. The negative anomaly then deepens nearly in-situ over Alaska, while slowly migrating southward toward the northern Gulf of Alaska. It is not until the key day that the center of the negative-height anomaly passes over the open

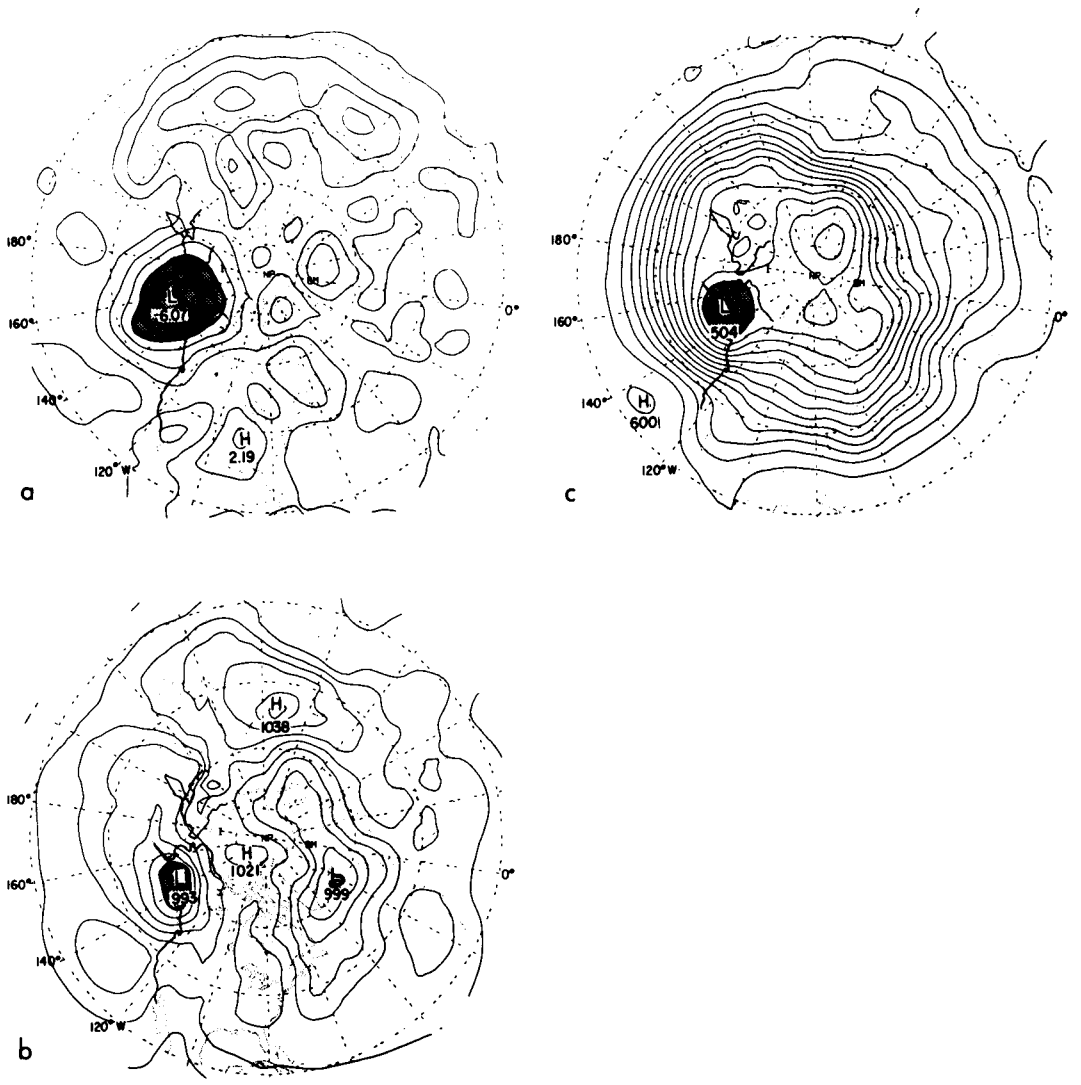

Fig. 11. Composite of 21 cases over the Gulf of Alaska, 1975–1983 for the key day: (a) 500 mb temperature anomaly field (contour interval 1 °C), (b) surface pressure composite (contour interval 4 mb), (c) 1000–500 mb thickness composite (contour interval 60 m).

water of the Gulf of Alaska. Following the key day, the negative anomaly slides southward and rapidly weakens.

Fig. 11a shows the 500 mb temperature anomaly field for the key day. A negative-temperature anomaly of more than 6 °C is centered slightly to the west of the negative-height anomaly over the Gulf of Alaska at this time. This temperature anomaly corresponds to a 500 mb temperature of less than −36 °C over a region where the mean sea-surface temperature is greater than 5 °C (Fig. 2). An air parcel warmed to near 5 °C at the ocean surface would result in a lifted index of ~−2 at 500 mb, indicating the potential for deep convection at the time polar lows form.

Surface-pressure gradients maintain a northerly flow across the Alaska Peninsula and Kodiak Island at the time the polar lows develop over the Gulf of Alaska (Fig. 11b). This flow direction is favorable for a rapid modification of the boundary-layer air as arctic air is advected over the warmer water south of the Alaska Peninsula (Fig. 2). The combined effects of the warming and moistening of the air at low levels and advection of very cold air aloft across the southern coast of Alaska likely results in destabilization of the troposphere.

The 1000–500 mb thickness composites (Fig. 11c) shows a pronounced thickness trough with several closed contours over the northern Gulf of Alaska on the key day. The thickness gradient is indicative of deeper baroclinicity and enhanced vorticity associated with the thermal wind on the larger-synoptic scale over this region.

5. Summary and conclusions

The two case studies presented in this paper show that the environments conducive to the development of strong polar lows include a deep outflow of arctic air over open water and a cold-core, closed low aloft. Additionally, differential PVA associated with a small-synoptic scale vortex at 500 mb may have provided a favorable environment in which the incipient vortices could develop into mature polar lows (Sutcliffe, 1947; Holton, 1979).

Calculations using sounding data suggest that the time scale needed for surface fluxes of sensible heat to modify the temperature profile of atmosphere below 850 mb is consistent with the time scale typically associated with the development of polar lows. Furthermore, the estimated warming of a column of air in the convective core of the polar-low as a result of sensible and latent heating can account for the deepening observed at the surface.

When synoptic conditions are favorable for the formation of polar lows, a series of storms can form in close proximity to each other during a relatively short time interval. Furthermore, once favorable conditions have developed these conditions may persist, resulting in the outbreak of polar lows over several days.

The superposed-epoch method of analysis used in this study has proven useful in examining the evolution of the 500 mb synoptic-scale height field just prior to and following the outbreaks of polar lows over the Gulf of Alaska. On days when well-developed polar lows occurred over this region significant negative-height and negative-temperature anomalies were present, indicating enhanced positive vorticity and a potential for deep convection over the area (Figs. 10f and 11a).

The surface-pressure composite (Fig. 11b) shows a trough of low pressure over the northern Gulf of Alaska, with northerly surface winds across the Alaska Peninsula and Kodiak Island, bringing arctic air into the Gulf of Alaska. As discussed in the case studies (Section 2), this flow direction is favorable for a modification of the boundary-layer air as it passes over water. The warming and moistening of the air at low levels, while very cold air aloft is advected across the Alaska Peninsula, likely results in a destabilization of the airmass.

The composite 1000–500 mb thickness field (Fig. 11c) shows a minimum just south of Kodiak Island, indicating the presence of deeper baroclinicity and enhanced vorticity associated with the thermal wind on the larger-synoptic scale over the Gulf of Alaska on the key day.

Comparing the compositing results for polar lows over the Gulf of Alaska with those over the Norwegian and Barents Seas (see Businger, 1985), the signature of the environments conducive to the formation of polar lows appear very similar in most of the variables studied for both regions. Strong negative-height and temperature anomalies were present at 500 mb on the key day in both regions. Low values of the 500–1000 mb thickness and low surface pressures were also present on the key day in both regions. One exception to the similarities, however, is the development of the significant positive-height anomaly along the east coast of Greenland in the study of polar lows over the Norwegian Sea. The magnitude and location of this feature have been attributed to topographic forcing by the high Greenland plateau and the Norwegian Sea. There is no counterpart to this positive-height anomaly in polar lows over the Gulf of Alaska. This difference is probably due to the difference in the geography of the two regions.

The evolution of the anomaly pattern over the Gulf of Alaska may have application in forecast-

ing polar lows in this region. The development of a deep trough over Alaska and the resulting northerly component of the flow aloft and at the surface over the northwestern Gulf of Alaska appear to precede the occurrence of polar lows. These conditions can be watched for in the NMC nested grid model to identify times during which the outbreak of polar lows is likely. The composite climatology may have application for analytical studies of the effects of sea surface forcing on the development of polar lows (Emanuel, 1986) and in providing initial conditions for primitive-equation models designed to simulate the evolution of polar lows.

6. Acknowledgements

The author wishes to thank Professor Richard Reed and Dr. Melvin Shapiro for helpful conversations, and Professor Peter V. Hobbs for his useful suggestions and editing of the manuscript. I am also grateful to Dr. Roy Jenne of the National Center for Atmospheric Research for his assistance in obtaining NMC data. I also wish to thank Kay Moore for drafting the figures. This material was based upon work supported by the National Science Foundation under Grant ATM-8306132 and the Office of Naval Research and Technology Directorate.

REFERENCES

Bjerknes, J. and Solberg, H. 1922. Life cycle of cyclones and the polar front theory of atmospheric circulations. *Geophys. Publ. 9*, 30–45.

Businger, S. 1985. The synoptic climatology of polar low outbreaks. *Tellus 37A*, 419–432.

Businger, S. 1986. *Cyclonic vortices in polar air masses.* Ph.D. Thesis, University of Washington.

Duncan, C. N. 1977. An investigation of polar lows. *Q. J. R. Meteorol. Soc. 103*, 255–268.

Eady, E. T. 1949. Long waves and cyclone waves. *Tellus 1*, no. 3, 33–52.

Emanuel, K. A. 1986. An air-sea interaction theory for tropical cyclones. Part I: steady-state maintenance. *J. Atmos. Sci. 43*, 585–604.

Harrold, T. W. and Browning, K. A. 1969. The polar low as a baroclinic disturbance. *Q. J. R. Meteorol. Soc. 95*, 710–723.

Holton, J. R. 1979. *Introduction to dynamic meteorology.* Academic Press, New York, 391 pp.

Jager, G. 1983. Satellite indicators of rapid cyclogenesis. *Mariners Wea. Log. 28*, 1–6.

Locatelli, J. D., Hobbs, P. V. and Werth, J. A. 1982. Mesoscale structures of vortices in polar air streams. *Mon. Wea. Rev. 110*, 1417–1433.

Mak, M. 1982. On moist quasi-geostrophic baroclinic instability. *J. Atmos. Sci. 39*, 2017–2027.

Mansfield, D. A. 1974. Polar Lows: The development of baroclinic disturbances in cold air outbreaks. *Q. J. R. Meteorol. Soc. 100*, 541–554.

Mullen, S. L. 1979. An investigation of small synoptic scale cyclones in polar airstreams. *Mon. Wea. Rev. 107*, 1636–1647.

Panofsky, H. A. and Brier, W. G. 1965. *Some applications of statistics to meteorology.* The Pennsylvania State University, 224 pp.

Rasmussen, E. 1977. The polar low as a CISK-phenomenon. *Report no. 6.* University of Copenhagen, Institute for Theoretical Meteorology.

Rasmussen, E. 1981. An investigation of a polar low with a spiral cloud structure. *J. Atmos. Sci. 38*, 1785–1792.

Rasmussen, E. 1983. A review of mesoscale disturbances in cold air masses. In *Mesoscale meteorology—theories, observations and models* (ed. D. K. Lilly and T. Gal-Chen). Reidel Publishing Co., 247–283, 781 pp.

Rasmussen, E. 1985a. A case study of a polar low development over the Barents Sea. *Tellus 37A*, 407–418.

Rasmussen, E. 1985b. A polar low development over the Barents Sea. *Technical Report No. 7.* The Norwegian Meteorological Institute, Oslo, Norway, 28 pp.

Rabbe, A. 1975. Arctic instability lows. *Meteorologiske Annaler 6*, 303–329.

Reed, R. J. 1979. Cyclogenesis in polar airstreams. *Mon. Wea. Rev. 107*, 38–52.

Reed, R. J. and Blier, W. 1986a. A case study of comma cloud development in the Eastern Pacific. *Mon. Wea. Rev. 114*, 1681–1695.

Reed, R. J. and Blier, W. 1986b. A further case study of comma cloud development in the Eastern Pacific. *Mon. Wea. Rev. 114*, 1696–1708.

Reed, R. J. and Duncan, C. N. 1987. Baroclinic Instability as a mechanism for the serial development of polar lows. *Tellus 39A*, 377–385.

Royer, T. C. 1975. Seasonal variations of waters in the northern Gulf of Alaska. *Deep Sea Res. 22*, 403–416.

Sardie, J. M. and Warner, T. T. 1985. A numerical study of the development mechanism of polar lows. *Tellus 37*, 460–477.

Satyamurti, P., Rao, V. B. and Moura, A. D. 1982. Subsynoptic-scale baroclinic instability. *J. Atmos. Sci. 39*, 1052–1061.

Shapiro, M. A. and Fedor, L. S. 1986. The arctic cyclone expedition, 1984: Research and aircraft

observations of fronts and polar lows over the Norwegian and Barents Sea, Part 1. *Polar lows Project, Technical Report No. 20.* The Norwegian Meteorological Institute, Oslo, Norway, 56 pp.

Shapiro, M. A., Fedor, L. S. and Hampel, T. 1987. Research Aircraft measurements within a polar low over the Norwegian Sea. *Tellus 39A*, 272–306.

Staley, D. O. and Gall, R. L. 1977. On the wavelength of maximum baroclinic instability. *J. Atmos. Sci. 34*, 1679–1688.

Sutcliffe, R. C. 1947. A contribution to the problem of development. *Q. J. R. Meteorol. Soc. 73*, 370–383.

Takioka, T. 1973. A stability study of medium-scale disturbances with inclusion of convective effects. *J. Meteorol. Soc. Japan 51*, 1–9.

Wallace, J. M. and Hobbs, P. V. 1977. *Atmospheric Science: an Introductory Survey.* Academic Press, 417 pp.

Zipzer, E. J. 1977. Mesoscale and convective-scale downdrafts as distinct components of squall-line structure. *Mon. Wea. Rev. 105*, 1568–1589.